ARTICLE NO. 80-4096

A 80-071

Specific Impulse Prediction of Solid-Propellant Motors

Ellis M. Landsbaum,* Manuel P. Salinas,† and J. P. Leary‡
The Aerospace Corporation, El Segundo, Calif.

The methods for the theoretical prediction of delivered specific impulse are relatively well known. They involve computing the losses due to two-phase flow, divergence, boundary layer, kinetics, nozzle submergence, and combustion inefficiency. The largest computed loss in typical aluminized solid propellants is the two-phase flow loss; this computation also has the largest uncertainty because the particle size and distribution are not precisely known. In this paper, a correlation of mean particle diameter vs throat diameter from experimental data was used with the solid-rocket performance prediction program to predict the propellant specific impulse of a number of motors. These predictions are compared to the experimental values. The results indicate that the specific impulse efficiency appears to be an inherent property of the propellant. In addition, the experimental specific impulse and specific impulse efficiency were statistically correlated against motor and propellant variables. These correlations are as accurate as the longer, more expensive, theoretical analysis. In addition to specific impulse prediction, the correlation equations are useful in optimization of motor designs.

Nomenclature

Al	= aluminum fraction
AP	= ammonium perchlorate
ASUB	= inlet area ratio
Bi	= binder fraction
c^*	= characteristic velocity, ft/s
D_p	= particle diameter, μm
D_t	= throat diameter, in.
F	= thrust, lb
I_{sp}	= specific impulse, s
L^*	= characteristic length, in.
L_n	= nozzle length, throat to exit, in.
P	= pressure, psi
r	= radius
R	= correlation coefficient
R_d	= radius of curvature, downstream, nondimensional (R/R_t)
R_t	= throat radius, in.
R_u	= radius of curvature, upstream, nondimensional (R/R_t)
S	= submergence fraction
TBL	= turbulent boundary layer, Eq. (7)
U	= velocity
$\dot{w}$	= weight flow, lb/s
β	= $(\tilde{\theta}+2\theta_e)/3$
δ^*	= displacement thickness
ϵ	= expansion ratio
η	= efficiency
θ	= momentum thickness
θ_i	= initial divergence angle, deg
θ_e	= exit angle, deg
$\tilde{\theta}$	= arctan $[D_t(\epsilon^{0.5}-1)/2L_n]$
λ	= $0.5+0.5\cos\beta$
ξ	= condensed phase, lb-mol/100 lb
ρ	= gas density
σ	= standard deviation

Superscript

0	= ideal

Subscripts

c	= combustion
k	= kinetic
o	= overall, measured
s	= submergence
2D2ϕ	= two-dimensional two-phase

Received July 25, 1979; revision received Jan. 2, 1980.

Index categories: Multiphase Flows; Engine Performance; Solid and Hybrid Rocket Engines.

*Manager, Solid Motors Section. Member AIAA.
†Member of the Technical Staff, Solid Motors Section.
‡Member of the Technical Staff, System Effectiveness Analysis Section.

Introduction

IT is highly desirable to be able to accurately predict the delivered specific impulse of solid propellants in rocket motors. This would assist in preventing unduly optimistic or conservative motor designs, in selecting solid propellants, in determining optimum motor parameters, and in selecting competing designs or alternatives. The methodology of solid rocket motor performance prediction is relatively well known; Cohen et al.[1] recently made an excellent review of the subject and assessed the accuracy of the predictions. In addition to specific impulse, that paper also considered ignition transients, peak pressures, tailoff, extinguishment, and the prediction of pressure-time traces. This paper will discuss only the prediction of delivered specific impulse.

Although there have been a large number of papers concerned with methodology, discussion of loss mechanisms, development of equations and computer programs, and the experimental determination of necessary data such as particle size, kinetic rates, drag coefficients, and heat-transfer coefficients, there have been very few papers that have compared experimental specific impulse measurements to analytical predictions. The first paper on that subject appears to be that of Kliegel and Nickerson,[2] who utilized the first program developed to calculate two-phase flow losses. The analysis estimated boundary layer and divergence losses, and was compared to experimental measurements on test motors designed to determine the adequacy of the analysis. The results were good. Additional studies comparing the predicted and experimental specific impulse have only appeared recently.[3-6] The predictive capability of these later studies is excellent with a maximum error of 0.6%. The motors analyzed were primarily small test motors containing double-base propellants. Twelve large test motors were analyzed as were four production motors.[4] Three of the production motors contained composite propellants. Composite

propellants were also studied in small test motors[5] with low expansion ratios (<10). Unfortunately, the programs utilized are not generally available. It is not clear how applicable Daines'[4] technique is to the range of composite propellants, motor and nozzle designs found in space motors—a large class of motors of considerable importance. A space motor is usually a motor of medium pressure, long burn time, and high expansion ratio. One study[7] has utilized empirical prediction techniques for these motors.

This study has two objectives, the first being to determine how well one could predict specific impulse, a priori. The second and more important objective was to determine how well one might predict motor performance if a limited amount of data were available on a motor of similar size or a near-identical motor with a different expansion ratio. These data are usually available because the conservatism of space systems usually dictates the use of proven technology. This study was to be accomplished by predicting the performance of a large sample of space motors for which the necessary information was available. The mechanics of the study were minimized by the availability of a solid performance prediction program (SPP) recently developed.[8] The following section gives a brief description of SPP. In subsequent sections, the motors are described and the results of the analysis presented. The experimental data is analyzed with a multivariable regression analysis, and equations giving delivered specific impulse and overall motor efficiency as a function of motor and propellant parameters are presented.

Description of SPP

SPP predicts delivered specific impulse based on the ideal value of specific impulse and losses in specific impulse due to the effects of two-phase flow, divergence, kinetics, boundary layer, submergence, and inefficient combustion. The program also has a general three-dimensional grain design capability and can predict mass flow, pressure, and thrust as a function of time, given the appropriate grain and motor dimensions and propellant ballistic properties. This portion of the program will not be discussed further. A brief description of the specific impulse prediction portion of the program will be offered to enable a better understanding and evaluation of the results to be presented later.

The delivered specific impulse is calculated using the following equation:

$$I_{sp}(\text{del}) = I^0_{sp}\eta_{2D2\phi}\eta_k\eta_s\eta_c - \Delta\text{TBL} \tag{1}$$

The terms are defined in the Nomenclature. The I^0_{sp} is the ideal vacuum specific impulse (ODE, one-dimensional equilibrium) calculated purely from thermodynamic data assuming one-dimensional flow, chemical equilibrium between species and phases, thermal and velocity equilibrium between condensed gaseous phases, and adiabatic isentropic flow. The program contains routines (subprograms) to calculate each of the efficiencies or losses in Eq. (1). Each of these routines will be described below.

The two-phase two-dimensional flow routine calculates combined two-phase and divergence efficiency ($\eta_{2D2\phi}$), and is based on the following assumptions and restrictions. The gas is an ideal gas with constant specific heats in the liquid and solid phase. Energy exchange between gas and particles occurs only by convection, and the only forces on the particles are viscous drag forces. The particle volume is negligible, and the internal temperature is uniform. The heat of condensation is accounted for. As many as nine particle groups of different diameters and weight fractions can be entered. The nozzle convergent section must be conical and less than 45 deg. The upstream and downstream radius of curvature at the throat can be different, but must be greater than 0.5 (normalized to the throat radii). There are five options for the exit cone: conical, parabolic, circular arc, and either a spline fit or straight tabular input. This routine calculates a two-dimensional, two-phase specific impulse, $I_{sp}(2D2\phi)$. It also calculates an ideal specific impulse, $I^0_{sp}(2D2\phi, \text{RE})$, using the same assumptions as in the ODE with the added restrictions of the two-dimensional, two-phase program. The two-dimensional two-phase efficiency is then calculated from the following equation:

$$\eta_{2D2\phi} = I_{sp}(2D2\phi)/I^0_{sp}(2D2\phi, \text{R.E.}) \tag{2}$$

This efficiency contains both the two-phase and divergence losses, and no attempt is made to separate them.

The kinetic efficiency (η_k) can be determined either by calculation or with an empirical equation. Both methods are described below. The kinetic loss calculation is one-dimensional. The same asumptions are made about the particles (condensed phase) as in the two-dimensional, two-phase portion of the program. Additionally, it is assumed that the particles are in thermal and velocity equilibrium with the gas. The gas can have a maximum of 150 distinct chemical reactions and 40 individual species. The maximum suggested for the C, H, O, N, Cl, Al system is 28 species and 73 reactions. Each reaction and the kinetic data must be input to the program so, typically, far less reactions are used. The program calculates a specific impulse, $I_{sp}(k)$, allowing for the effects of the kinetic reactions. It also calculates an ideal specific impulse, $I^0_{sp}(k, \text{R.E.})$, using the assumptions of ODE and the additional assumptions about particle equilibrium used in the kinetic calculation. The gas species are allowed to vary according to equilibrium requirements, so one should input sufficient information to cover the major species and reactions. The specific impulse efficiency is then calculated from the ratio of these two specific impulses as follows:

$$\eta_k = I_{sp}(k)/I^0_{sp}(k, \text{R.E.}) \tag{3}$$

The results to be discussed later did not determine a kinetic efficiency by calculation but, instead, used the empirical formula. The empirical loss is based on the difference between frozen composition (ODF) and equilibrium specific impulse with a pressure correction. The equation is

$$\eta_k = 1 - 0.333\left[1 - \frac{I^0_{sp}(\text{ODF})}{I^0_{sp}(\text{ODE})}\right]\frac{200}{P} \qquad (P \geq 200) \tag{4}$$

Later, the differences between calculated and empirical kinetic efficiencies will be discussed.

A semiempirical equation for submergence loss is provided within SPP. The equation is

$$\eta_s = 1 - 0.000684[P\xi/\text{ASUB}]^{0.8} S^{0.4} D_t^{-0.2} \tag{5}$$

A complex empirical equation for combustion efficiency as a function of propellant composition and burn rate is provided. The calculations described herein assumed 100% combustion efficiency; therefore, the efficiency function is not presented. It is probably better to base an estimate of the combustion efficiency on experimental information or experience, if available, than to use that provided by SPP which, in addition to its complexity, may not be particularly accurate.

The boundary-layer loss (ΔTBL) is calculated from the turbulent boundary-layer (TBL) routine. This is an integral method that uses the boundary-layer edge conditions from the two-dimensional, two-phase flow program. Although it is considered inaccurate for heat-transfer calculations, particularly at the throat region, it appears to be sufficiently accurate for the thrust loss calculation considering the small loss. The thrust loss is determined from the momentum deficit in the boundary layer at the nozzle exit plane from the following:

$$\Delta F_{\text{BL}} = 2\pi r\rho U^2\theta\cos\theta_e\left[1 - \frac{\delta^* P}{\theta\rho U^2}\right] \tag{6}$$

Table 1 Motor data

Motor No.	Mfg. No.	Propellant			Nozzle							Sub, %	$\bar{D}_t$ (in.)	$\bar{\epsilon}$	$\bar{P}$ (psia)
		Binder	% AP	% Al	Type	ASUB	R_d	R_u	θ_i (deg)	θ_e (deg)	L_n (in.)				
1	SVM-1	CTPB	73	15	parabola	3.30	2.0	2	27	16.8	15.0	3	2.32	33.3	377
2	SVM-2	CTPB	73	15	parabola	2.65	1.7	2	27	16.1	16.4	24	2.75	28.0	322
3	SVM-4A	CTPB	73	15	wall	3.61	2	2	25	16.5	25.1	0	3.43	40.0	731
4	SVM-5	CTPB	73	15	parabola	3.55	0.9	1	27	15.6	15.3	24	2.61	26.8	515
5	SVM-6	CTPB	73	15	parabola	4.64	1	1	31	14.9	24.6	0	2.84	54.0	602
6	SVM-7	CTPB	73	15	parabola	2.64	1.4	2.1	31.5	14.3	28.3	24	3.27	51.2	612
7	MM III, st. 2	CTPB	73	15	parabola	2.42	1	2	26.7	16.7	52.6	14	9.63	24.8	443
8	MM III, st. 3	CTPB	73	15	arc	2.42	2	1	29	13.6	35.1	29	6.88	23.6	507
9	MM III, st. 3 W/EEC(ASPC)	CTPB	73	15	wall	2.42	2	1	29	17	54.0	29	6.88	42.7	507
10	MM III, st. 3 W/EEC(HPC)	CTPB	73	15	wall	2.42	2	1	29	20	76.0	29	6.88	87.9	523
11	FW-4	PBAN	68	16.4	conical	2.70	2	2	20	20	19.9	9	2.41	47.3	683
12	FW-5	PBAN	68	16.4	conical	2.80	1.7	2	19.9	19.9	19.2	9	2.12	55.6	670
13	FW-5A	PBAN	68	16.4	conical	2.80	1.7	2	19.7	19.7	26.2	9	2.10	96.9	733
14	IUS	HTPB	68	18	arc	3.48	1.0	2	27	14.7	44.8	38	7.09	33.1	549
15	364-3	CTPB	70	16	wall	2.85	0.86	2	24.5	14.1	28.8	45	3.36	51.2	568
16	364-4	CTPB	70	16	wall	2.29	0.78	2	23.3	13.6	27.2	43	4.36	29.8	545
17	364-11	CTPB	72	16	wall	2.31	0.89	2	23.9	14	27.9	26	4.24	32.1	547
18	364-19	CTPB	70	16	wall	2.48	0.81	2	23.7	12.8	27.8	31	3.82	39.3	588
19	442-1 (a)	CTPB	69	16	conical	1.92	1	2	20	20	13.2	40	2.99	17.5	642
20	479	CTPB	70	16	wall	2.53	1.1	2.1	23.7	14.2	13.0	26	1.44	55.0	788
21	521	CTPB	70	16	wall	3.07	0.85	1	24.3	13.9	16.8	19	1.93	50.7	645
22	604	CTPB	70	16	wall	3.72	0.5	1	26.7	14.1	17.1	10	2.50	35.4	485
23	616	CTPB	72	16	wall	2.87	1	1	24.5	14.8	21.8	18	2.82	46.0	465
24	640	CTPB	70	16	conical	2.70	2	2	20.0	20.0	19.9	9	2.41	47.0	676
25	714-1	HTPB	71	18	wall	2.61	1	2	24	14.6	34.4	26	3.57	64.6	609
26	714-2	HTPB	59	20	wall	2.76	0.91	2	24	14.6	34.6	27	3.32	74.7	723
27	Y41-4	PBAA	69	16	conical	4.89	2	2	15	15	15.0	21	1.35	40.2	367
28	Y41-7	PBAA	69	16	conical	4.89	2	2	15	15	30.0	21	1.36	149.3	356
29	258-E6 (b)	Double Base	7	19	conical	2.45	2	2	18	18	20.0	6	3.16	25.1	454
30	259-A6 (b)	Double Base	7	19	conical	1.65	2	2	15	15	41.1	6	6.67	17.9	344

(a) Contains 1% Fe_2O_3 (b) Initial nozzle dimensions

Table 2 Performance data

Motor No.	$I_{sp}o$	I_{sp} del	I_{sp} pred	ΔI_{sp}	η_o	$\eta_{2D2\phi}$	η_s	η_k	ΔTBL
1	312.0	288.3	286.4	-1.9	0.9240	0.9339	0.9978	0.9923	2.2
2	308.7	284.0	283.4	-0.6	0.9200	0.9375	0.9950	0.9910	2.0
3	315.6	289.7	290.9	+1.7	0.9163	0.9303	1.0	0.9964	1.7
4	308.4	281.2	285.1	+3.9	0.9118	0.9409	0.9941	0.9949	1.8
5	320.2	293.2	297.8	+4.6	0.9157	0.9415	1.0	0.9953	2.2
6	319.4	293.6	295.6	+2.0	0.9192	0.9443	0.9917	0.9954	2.1
7	306.8	287.6	286.7	-0.9	0.9374	0.9486	0.9956	0.9940	1.3
8	306.0	284.7	284.5	-0.2	0.9304	0.9464	0.9929	0.9949	1.6
9	316.4	293.0	294.8	+1.8	0.9260	0.9492	0.9929	0.9944	1.7
10	327.0	300.3	301.6	+1.3	0.9183	0.9400	0.9927	0.9942	1.7
11	315.8	286.2	289.2	+3.0	0.9063	0.9310	0.9934	0.9962	1.7
12	318.2	286.5	291.1	+4.6	0.9004	0.9304	0.9934	0.9960	1.9
13	325.8	293.1	297.8	+4.7	0.8996	0.9309	0.9929	0.9962	2.1
14	312.3	287.7	289.1	+1.4	0.9212	0.9418	0.9929	0.9950	1.5
15	317.1	290.7	291.5	+0.8	0.9168	0.9393	0.9902	0.9953	2.0
16	308.5	284.6	284.4	-0.2	0.9225	0.9416	0.9895	0.9954	1.6
17	311.1	289.5	287.9	-1.6	0.9306	0.9441	0.9914	0.9950	1.8
18	313.0	288.9	288.3	-0.6	0.9230	0.9397	0.9906	0.9956	1.8
19	294.9	272.8	271.1	-1.7	0.9251	0.9339	0.9855	0.9966	1.2
20	318.3	290.0	290.2	+0.2	0.9111	0.9347	0.9867	0.9968	2.4
21	317.0	288.6	290.8	+2.2	0.9104	0.9361	0.9919	0.9960	2.3
22	311.3	285.9	286.6	+0.7	0.9184	0.9361	0.9960	0.9946	2.1
23	317.1	290.2	290.9	+0.7	0.9152	0.9359	0.9941	0.9936	2.2
24	315.9	288.3	289.7	+1.4	0.9126	0.9318	0.9936	0.9962	1.7
25	324.8	296.8	298.1	+1.3	0.9138	0.9385	0.9904	0.9949	2.3
26	329.7	298.1	301.6	+3.5	0.9042	0.9364	0.9887	0.9955	2.3
27	309.7	282.7	283.5	+0.8	0.9128	0.9345	0.9960	0.9931	2.7
28	325.7	294.3	294.8	+0.5	0.9036	0.9255	0.9961	0.9923	3.1
29	298.9	281.7	276.2	-5.5	0.9425	0.9370	0.9960	0.9956	1.5
30	292.6	281.4	273.9	-7.5	0.9617	0.9500	0.9962	0.9942	1.4

Specific impulse losses are determined by dividing the thrust loss by the mass flow from the two-dimensional two-phase routine.

$$\Delta\text{TBL} = \Delta F_{\text{BL}} / \dot{w}_{2D2\phi} \quad (7)$$

Motor Data and Analysis Method

Sufficient information was obtained from motor manufacturers to allow the analysis of the 30 motors listed in Table 1. The motors are numbered to allow easy comparison with the results given in Table 2 and for ease of discussion. The propellant information indicates the type of binder and weight percent of ammonium perchlorate and aluminum, while the nozzle type shows whether it is conical, parabolic, (circular) arc, or wall, indicating that a wall table was used for some other type of contour. ASUB is the ratio of the inlet nozzle area to the initial throat area. The inlet area was based on the nose of the convergent section of the nozzle; analysis shows that large changes in this value only affect the submergence efficiency. The radii of curvature at the throat are those for the initial contour. The initial deflection angle downstream of the throat is θ_i, while θ_e is the exit angle determined by the routine and is discussed below. Nozzle length is the initial nozzle length from throat to exit plane, submergence is the submerged length of the nozzle divided by the grain length, and throat diameter is the average of the initial and final throat diameters. The average expansion ratio is based on the initial exit area and the throat area calculated from the average throat diameter. The average pressure is that over web burn when there is a sharp tailoff. If there is no obvious web burnout, then the average pressure over action time is given. Action time is the time between pressures that are 10% of maximum chamber pressure.

Using the initial radius of curvature (R_d) with the average throat radius results in slight differences between the analyzed and original nozzle contours. The conical nozzles analyzed become slightly shorter than the original. The nozzle length of the circular arc and parabolic contours was fixed, as was θ_i; the result is a slightly smaller exit angle than the original contour. The nozzles with tabulated wall contours had to be adjusted slightly to allow a smooth transition from the circular arc to the contour. These slight alterations in contour should have a negligible effect on the calculated specific impulse. This was considered preferable to using the initial contour and trying to correct the calculated specific impulse for the change in expansion ratio and also for the effect of the change in throat diameter on the particle size.

This analysis used a mean particle diameter that was a function of throat diameter only, as shown in Fig. 1. This is the result of some early work of Delaney on the measurement of mean particle diameters. The final correlation of Delaney[9] is also shown in the figure. The earlier correlation was used because of previous analyses that indicated its use in the predecessor programs to SPP gave predicted specific impulses that agreed rather well with experimental values for a number of motors. The correlation in the SPP is also shown in Fig. 1, and the equation is given below:

$$D_p = 0.454\, P^{1/3} \xi^{1/3} [1 - \exp(-0.0004 L^*)](1 + 0.045\, D_t) \quad (8)$$

This correlation was not used because of the smaller particle size it predicts. Only a single particle size was used, as analyses have indicated that there is a negligible effect of using multiple particle sizes. Multiple particle sizes are primarily of interest in studying possible impingement. A particle density of 168 lb/ft^3 (2.69 g/cm^3) was used, equivalent to a temperature of 4600°R (2556 K). With single particles, very few of the particles ever solidify, and this is a representative particle density. Some interaction between the particle density and particle size on the results of the calculation is recognized. An inlet angle of 30 deg was used which will normally not result in impingement with SPP. Therefore, impingement losses were not considered.

Analysis Results and Discussion

The results of the analysis are presented in Table 2. The theoretical (ODE) vacuum specific impulse, I_{sp}^0, was calculated under the conditions ($\bar{\epsilon}, \bar{P}$) given in Table 1. This calculation is made at a propellant temperature of 25°C. The delivered specific impulse is the experimental measurement made at simulated altitude conditions and corrected to vacuum conditions, and is the total impulse delivered by the motor divided by the loaded propellant weight. The data are reported at a variety of propellant temperatures near ambient. The correction for temperature is so small, approximately 0.015 s/°F, that it can be neglected. The predicted specific impulse is calculated as previously described. The error in the prediction, ΔI_{sp} (predicted specific impulse minus delivered specific impulse) is given. The overall efficiency (η_o) is delivered specific impulse divided by the theoretical one-dimensional value. The remaining columns are the efficiencies and boundary-layer loss calculated by the program.

A plot of the predicted vs delivered specific impulse is shown in Fig. 2. It will be noted immediately that one tends to overpredict the specific impulse. A gross underprediction is made for motors 29 an 30 with double-base propellant. If average values for the nozzles of these motors had been available instead of the initial conditions used, the errors would have been larger. Most of the ensuing discussion will neglect these two motors because they contain double-base propellants, and their experimental results (I_{sp}(del),η_o) are statistically different from the other motors containing composite propellants.

The average error (ΔI_{sp}) for the 28 composite propellant motors in Table 2 is 1.2 s. The standard deviation is 1.9 s

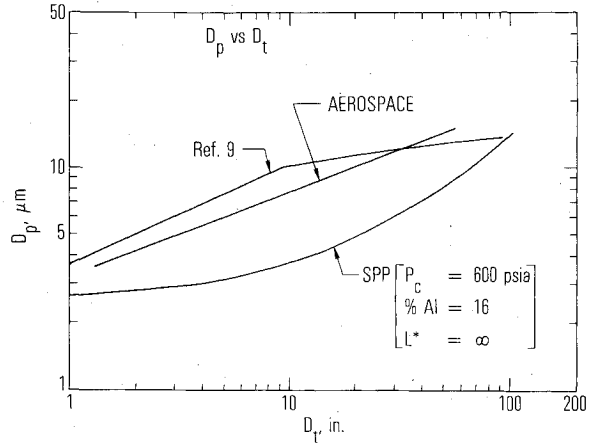

Fig. 1 D_p **vs** D_t.

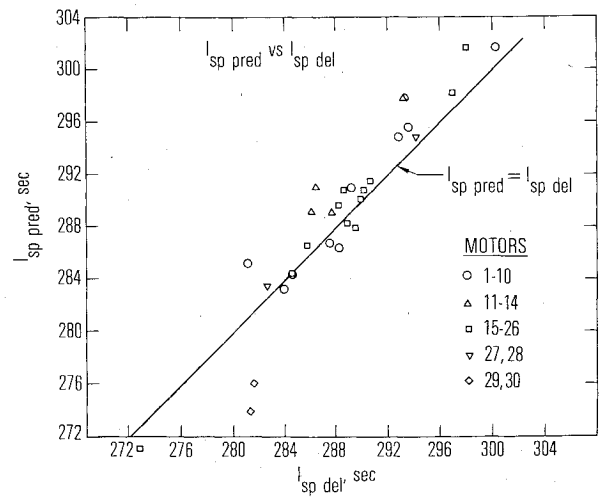

Fig. 2 I_{sp}**(pred) vs** I_{sp}**(del).**

—undesirably high. Possible causes of the error will be discussed later. These results are clearly less accurate than desirable. There is another question that requires examination. Given firing data, how well can one predict the performance of a higher expansion ratio nozzle or of a similar motor from the same family? In these cases, the analysis provides much better results. Compare motor 27 and 28 and motor 12 with 13, where identical motors were fired with different expansion ratios. Given the results of the firing of the low expansion ratio motor and applying the bias between the predicted and experimental values of specific impulse for that motor to the prediction of the high expansion ratio motor, very accurate results are obtained. Thus, given the results of motor 12, one would have predicted motor 13 within 0.1 s and, given the results of motor 27, one would have predicted motor 28 within 0.3 s. The results for the Minuteman motors with extendable exit cones (EEC) are less accurate. However, cones were not extended over the full duration of the firings, and there were some minor problems with the cones that may have reduced the specific impulse slightly. Therefore, this procedure can be considered to be very accurate.

Noting how similar the biases are for similar motors, one finds relatively good agreement. Thus, motors 4 and 5 are similar, as are motors 15, 16, and 18 and motors 20, 21, and 22; within each group biases are quite similar. The worst spread of biases within each group is 2 s. This would indicate that with data from one motor, one should be able to predict a similar motor within 2 s. A larger view may also be taken of the group of motors, and one finds that the CTPB propellant motors (15-24) are grouped closely as are the PBAN motors (11-13). The SVM motors (1-6) can be divided into two groups—low- and high-pressure motors—and each group has a relatively small spread in bias. Thus, it appears that, given data for a single motor, one can predict similar motors within approximately 2 s.

A limited number of kinetic efficiencies were calculated to compare with the empirical values [Eq. (4)]. They only included 11 gaseous species (H, OH, H_2O, O, O_2, H_2, CO_2, CO, N, N_2, NO), 8 recombination reactions, and 15 binary exchange reactions. This limited analysis indicates that the empirical kinetic equation underestimated the loss at the higher pressures (greater than 300 psi) by approximately 0.5%. It also appears that a better pressure correlation in Eq. (4) would be $300/P$ rather than $200/P$. The boundary-layer routine was run with an adiabatic wall. If a colder wall had been used, representative of the nozzle temperature, the boundary-layer loss would have increased slightly. These corrections would reduce the bias from 1.2 s to approximately −1 s. Impingement was not considered in the analysis but, reportedly, all of the motors have negligible impingement, except for motor 14 for which a preliminary estimate is that the loss due to the impingement is approximately only 1 s.

It is unlikely that the errors in the specific impulse prediction are due to errors in the submergence, kinetics, or boundary-layer losses as the motors and propellants are too similar to allow much variation in these losses. The errors must be due to the assumption of 100% combustion efficiency or to the particle correlation used. A measure of combustion efficiency would be the c^* efficiency. Although specific impulse measurements are readily available, c^* measurements are not typically reported. An attempt will be made to obtain this information to see if the accuracy of the prediction is improved. The introduction of a pressure term into the particle size correlation, such as in Eq. (8), would probably improve the analysis. This is best illustrated by considering the SVM motors (1-6) where introduction of particle size as a function of pressure would reduce the error between the low- and high-pressure motors. The particle size may also be dependent on the propellant properties, as evidenced by the high efficiency of the double-base motors (29-30). Motor 11 and 24, identical except for the propellants and with a difference in efficiency of 0.6%, may also be compared. However, motor 24 has had only a single altitude firing. The only method for predicting particle size other than the correlation discussed herein is the method of Bartlett and Delaney[10] utilized by Daines.[4] The authors have not yet tried this technique. It is doubtful that this technique would result in sufficiently different particle sizes, given the similarity of the propellants and the limitation of the program to conical inlets. The particle size may be a complex function of propellant properties and motor conditions not readily identified. Inclusion of measured c^* efficiencies in the analysis may indicate the extent to which particle size prediction is in error.

Statistical Analysis

The experimental data for the motors containing composite propellants were statistically analyzed with a multivariable least-squares regression analysis to determine if useful correlations for preliminary estimates or optimization programs could be developed. The data from motors 1-28, except for motor 19, were used. Motor 19 was eliminated because previous analyses[11] had shown it to be a large outlier in correlating overall efficiency η_o. Motor 19 contains the only propellant with substantial iron oxide. Also, it has the lowest expansion ratio of any of the motors and had only one test firing. Primary emphasis was given to correlating η_o as it gave a smaller error than I_{sp}.

The statistical analysis was conducted in three parts: 1) the form of the equation to be used was determined, 2) the variables to reflect divergence loss were selected, and 3) all the significant variables were determined.

The equations studied were

$$\eta_o = \lambda \cdot \Sigma a_i \ell n x_i \tag{9}$$

$$\eta_o = \Sigma a_i \ell n x_i \tag{10}$$

$$\ell n \eta_o = \Sigma a_i \ell n x_i \tag{11}$$

where only the variables $\bar{D}_t$, $\bar{\varepsilon}$, Al, 1-S, and λ were considered. The previous study[11] had identified these as significant. The natural logarithms of the independent variables were used because earlier studies of two-phase flow with one-dimensional analysis showed the efficiency could be correlated by an equation of this form. The submergence was entered as 1-S to prevent mathematical difficulties with zero submergence. The divergence efficiency was previously used by Kirschner.[7] Correlations with standard deviations were obained using each of the equations. The standard deviations were 0.00347, 0.00321, and 0.00349 for Eqs. (9), (10), and (11), respectively. Equation (10) was used in subsequent analysis as it had the lowest sigma.

The best variable for divergence loss was then determined. The criteria used was: Which variable gave the lowest sigma? It was found that β was slightly better than λ and that θ_i was not significant. When the angles $\bar{\theta}$ and θ_e were used (components of β), $\bar{\theta}$ was not significant, and the result with θ_e was inferior to that using β. Thus, β was selected to represent divergence losses.

Aluminum fraction was changed from a logarithmic to a linear variable before further analysis was done. It was noted that the coefficient for Al fraction in Eq. (10) would not allow extrapolation outside the limits of the experimental data. Also, two-phase flow losses were expected to be directly proportional to aluminum content.

The analysis was then expanded to include the other variables of Table 1: ASUB, R_u, R_d, $\bar{P}$, and binder fraction Bi. Variables were added to the equation in the order in which they reduced the mean-square error in a single-variable equation. In practice, it is simpler to first include all of the variables in a correlation. Then the coefficient for each variable is tested with a student "t" test for the null

hypothesis that the coefficient is equal to zero. The variables are then ranked. The most important variable is the one with the lowest probability of a zero coefficient. Variables are added if they reduce the mean-square error. Typically, this includes all variables for which the probability is less than 10% that the coefficient is zero.

The final equation with the lowest mean-square error is

$$\eta_o = 1.1336 + 0.0122\ \ell n\ \bar{D}_t - 0.0465\ \ell n\ \beta - 0.230\ \text{Al} - 0.0048\ \ell n\ \bar{\epsilon} + 0.0153\ \ell n(1-S) - 0.00842\ \ell n\ \text{ASUB} - 0.00548\ \ell n\ \bar{P} + 0.0033\ \ell n\ R_u$$

$$\sigma = = 0.00277 \qquad R = 0.968 \qquad (12)$$

The variables are in order of significance. Testing the probability of accepting the null hypothesis that the regression coefficients are equal to zero gave the following values: $<2\times10^{-5}$, 0.0035, 0.1, 1, 1, 3.5, 8, and 10% for $\bar{D}_t$, β, Al, $\bar{\epsilon}$, $1-S$, ASUB, $\bar{P}$, and R_u, respectively. Not significant were R_d and binder content. The number of variables can be reduced at the expense of a slight increase in σ

$$\eta_o = 1.0605 + 0.0111\ell n\bar{D}_t - 0.0328\ell n\beta - 0.254\text{Al} - 0.00617\ell n\bar{\epsilon}$$

$$\sigma = 0.00342 \qquad R = 0.940 \qquad (13)$$

Obviously, one may also use Eq. (12) with typical values for the less-significant variables.

The results of correlating overall efficiency produce an error (1σ) of 0.3% [Eq. (12)], a very acceptable figure. The statistical analysis reduces the error significantly since the variation (1σ) in the experimental value of η_o is 1.0%. The mean of η_o is 0.9164. Statistical analysis of efficiency resulted in a smaller error in predictions than the more exact calculation (SPP) which had a 1σ error of 0.65% (1.9 s). The developed correlation equations are admirably suited for preliminary analysis and optimization studies.

An identical statistical analysis was carried out for delivered specific impulse. However, the final significant variables were different. The equation giving the lowest mean-square error is

$$I_{sp}(\text{del}) = 216.9 + 11.5\ \ell n\bar{\epsilon} + 3.00\ \ell n\ \bar{D}_t - 11.7\ \ell n\ \text{Bi} + 5.05\ \ell n\ \theta_i + 1.66\ \ell n\ R_u - 4.46\ \ell n\ \theta_e + 3.52\ \ell n(1-S) - 2.13\ \ell n\ \text{ASUB}$$

$$\sigma = 1.14\text{s} \qquad R = 0.979 \qquad (14)$$

The probability of accepting the null hypothesis is $<2\times10^{-6}$, 0.06, 0.1, 3.5, 6, 8.5, 15, and 15% for $\bar{\epsilon}$, $\bar{D}_t$, Bi, θ_i, R_u, θ_e, $1-S$, and ASUB, respectively. The Bi is the binder fraction. Note that Al and P are not significant, and the divergence loss variables are different. Using β gave a slightly larger σ. Again, the number of variables can be reduced, resulting in a slightly larger σ.

$$I_{sp}(\text{del}) = 203.7 + 11.0\ \ell n\ \bar{\epsilon} + 2.74\ \ell n\ \bar{D}_t - 13.6\ \ell n\ \text{Bi} + 4.10\ \ell n\ \theta_i$$

$$\sigma = 1.30\ \text{s} \qquad R = 0.967 \qquad (15)$$

The efficiency equation should be more useful than the specific impulse equation because it has a lower error, and extrapolation to conditions outside the range of variables considered is more likely to be satisfactory. The specific impulse equations were primarily developed for a quick estimation and will not be commented upon further.

The coefficients and variables of Eq. (12) deserve further comment. That $\bar{D}_t$ is the most significant variable is not surprising considering the dependence of particle diameter on throat diameter and its affect on two-phase flow losses, the major loss mechanism. With D_t as the only variable, the mean-square error of the experimental data is reduced by 52%. The coefficient for β appears large; however, the change in η_o between a 15- and 20-deg nozzle is -0.013, very close to the -0.014 from λ. The $\Delta\eta_o$ for 0.16 Al is 0.037, only slightly smaller than expected. The coefficient of $\bar{\epsilon}$ is considerably less than one previously used that resulted from a one-dimensional analysis. A submergence (S) of 0.25 is an efficiency loss of 0.0044, less than the 0.006 of Kordig and Fuller[12] and about half that of SPP. The negative coefficient of pressure is as expected if the particle size increases with pressure as in SPP [Eq. (8)]. However, note that large pressure changes have a negligible effect on efficiency. The appearance of ASUB and R_u are surprising since their variation in SPP has a negligible effect, less than that in Eq. (12). According to Eq. (12), a short entrance with high R_u is desirable. The absence of R_d is surprising, especially since Daines[6] found it significant in his theoretical studies.

Conclusion

Data were obtained on a large number of space motors, and delivered specific impulse predictions were made and compared to the experimental values. The calculations were made with the recently developed solid-rocket performance prediction program. The error was not as small as would be desirable. The result was an average bias of 1.2 s and a standard deviation of 1.9 s. Prediction of specific impulse of a motor from experimental data on a similar motor is more accurate. The prediction of specific impulse for a high expansion ratio using the data for the same motor with a lower expansion ratio is very accurate.

Delivered specific impulses and specific impulse overall efficiencies were correlated against the motor and propellant variables. Not all variables were found to be significant. The error for the delivered specific impulse correlations was better (0.3%) than that of the detailed analysis (0.65%). The correlation of efficiency η_o had an error of only 0.30% and the coefficients in general agreed with theoretical predictions. The efficiency correlation is more useful than the specific impulse correlation, as extrapolation to conditions outside the range of variables tested is more likely to be satisfactory. The statistical correlations developed are very useful for preliminary estimates and motor optimizations.

Note Added in Proof: An error was discovered in the original calculations for motors 29 and 30. The correct values in Table 2 for motors 29 and 30 respectively are $I^0_{sp} = 304.9$ and 297.5 s, $\Delta I_{sp} = -1.8$ and -3.6 s and $\eta_o = 0.9239$ and 0.9459. The other losses are essentially identical. Thus, the efficiency of these motors containing double-base propellant is similar to that of the other motors with composite propellants.

Acknowledgments

This study was supported by the Air Force Space and Missile Systems Organization under Contract No. F04701-78-C-0079.

References

[1] Cohen, N.S., Harry, D.P., III, Price, C.F., Coats, D.E., Levine, J.N., and Nickerson, G.R., "Solid Rocket Performance Prediction Techniques," AIAA Paper 74-1200, AIAA/SAE 10th Propulsion Conference, Oct. 1974.

[2] Kliegel, J.R. and Nickerson, G.R., "Flow of Gas-Particle Mixtures in Axially Symmetric Nozzles," *Progress in Astronautics and Rocketry, 6: Detonation and Two-Phase Flow,* Academic Press, New York, 1962, pp. 173-194.

[3] Daines, W.L., Boardman, T.A., Lund, R.K., and Abel, R., "Effect of Aluminum Oxide Impingement on Specific Impulse of Solid Propellant Rocket Motors," AIAA Paper 76-145, AIAA/SAE 12th Propulsion Conference, July 1976.

[4] Daines, W.L., Mayberry, J.L., Lund, R.K., and Abel, R., "Prediction of Thrust Losses Occurring in Solid-Propellant Rocket Motors," AIAA Paper 74-1201, AIAA/SAE 10th Propulsion Conference, Oct. 1974.

[5] Daines, W.L. and Boyd, D.L., "Effect of Aluminum Concentration in Propellant on Performance of Rocket Motors," AIAA Paper 74-1277, AIAA/SAE 11th Propulsion Conference, Sept. 1974.

[6] Lavery, J.R., Abel, R., Lund, R.K., and Daines, W.L., "Experimental Investigation of the Effects of Internal Nozzle Contouring on Nozzzle Performance," *JANNAF Propulsion Meeting,* 1974 (CPIA Pub. 260), Vol. III, Pt. 2, Oct. 1974, pp. 623-643.

[7] Kirschner, T.J., Jr., "Prediction of Delivered Specific Impulse Using Empirical Techniques," *JANNAF Propulsion Meeting,* 1975 (CPIA Pub. 266), Vol. III, Oct. 1975, pp. 115-134.

[8] Coats, D.E., Levine, J.N., Nickerson, G.R., Tyson, T.J., Cohen, N.S., Harry, D.P., III, and Price, C.F., "A Computer Program for the Prediction of Solid Propellant Rocket Motor Performance," AFRPL-TR-75-36, Vol. I, July 1975.

[9] "Solid Rocket Motor Performance Analysis and Prediction," NASA SP-8-39, May 1971, p. 24.

[10] Bartlett, R.W. and Delaney, L.J., "Effect of Liquid Surface Tension on Maximum Particle Size in Two-Phase Flow," *Pyrodynamics,* Vol. 4, 1966, pp. 337-341.

[11] Landsbaum, E.M. and Salinas, M.P., "Solid Propellant Specific Impulse Prediction," AGARD Symposium on Solid Rocket Motor Technology, Oslo, Norway, April 1979.

[12] Kordig, J.W. and Fuller, G.H., "Correlation of Nozzle Submergence Losses in Solid Rocket Motors," *AIAA Journal,* Vol. 5, Jan. 1967, pp. 175-177.